Polymer 51 (2010) 5236–5244

Contents lists available at ScienceDirect

Polymer

journal homepage: www.elsevier.com/locate/polymer

Nanocomposites of poly(ether ether ketone) with carbon nanofibers: Effects of dispersion and thermo-oxidative degradation on development of linear viscoelasticity and crystallinity

Shriraj H. Modi [a,b], Kimberly B. Dikovics [a,b,1], Halil Gevgilili [a], Gaurav Mago [c], Stephen F. Bartolucci [d], Frank T. Fisher [c], Dilhan M. Kalyon [a,b,*]

[a] Highly Filled Materials Institute, Stevens Institute of Technology, Hoboken, NJ 07030, USA
[b] Department of Chemical Engineering and Materials Science, Stevens Institute of Technology, Hoboken, NJ 07030, USA
[c] Department of Mechanical Engineering, Stevens Institute of Technology, Hoboken, NJ 07030, USA
[d] U.S. Army Benét Laboratories, Armaments Research Development and Engineering Center, Watervliet, NY 12189-4000, USA

ARTICLE INFO

Article history:
Received 9 June 2010
Received in revised form
20 August 2010
Accepted 27 August 2010
Available online 6 September 2010

Keywords:
PEEK
Nanocomposites
Carbon nanofibers

ABSTRACT

Poly(ether ether ketone), PEEK, is a widely used engineering plastic that is especially suitable for high temperature applications. Compounding of PEEK with carbon nanofibers, CNF, has the potential of enhancing its mechanical and thermal properties further, even at relatively low CNF concentrations. However, such enhancements can be compromised by myriad factors, some of which are elucidated in this study. Considering that the dispersion of the CNF into any high molecular weight polymer is a challenge, two different processing methods, i.e., melt and solution processing were used to prepare PEEK nanocomposites with low aspect ratio carbon nanofibers. The linear viscoelastic material functions of PEEK nanocomposites in the solid and molten states were characterized as indirect indicators of the dispersion state of the nanofibers and suggested that the dispersion of nanofibers into PEEK becomes difficult at increasing CNF concentrations for both solution and melt processing methods. Furthermore, the time-dependence of the linear viscoelastic material functions of the PEEK/CNF nanocomposites at 360–400 °C indicated that PEEK undergoes thermo-oxidative cross-linking under typical melt processing conditions, thus preventing better dispersion by progressive increases of the mixing time and specific energy input during melt processing. The crystallization behavior of PEEK is also affected by the presence of CNF and degree of cross-linking, with the rate of crystallization decreasing with increasing degree of cross-linking and upon the incorporation of CNFs both for the solution and melt processed PEEK nanocomposites.

1. Introduction

Poly(ether ether ketone), or PEEK,

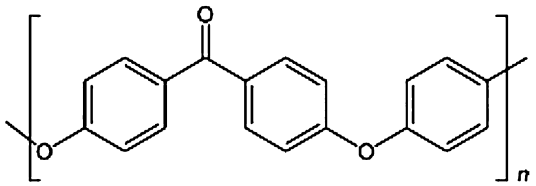

is an engineering plastic that is widely used especially in aerospace, automotive and health care applications [1,2] because of its superior mechanical and chemical properties [3]. PEEK has a glass transition temperature of 143 °C and a melting temperature of approximately 343 °C [4]. Such high transition temperatures permit its utilization at relatively high temperatures, but also require processing at correspondingly high temperatures, i.e., typically >360 °C, at which the degradation of PEEK becomes an issue.

The thermal degradation behavior of PEEK has been investigated under a variety of conditions [4–9]. These studies have generally kept PEEK at different temperatures for differing durations of time and then analyzed the resulting structure and properties. Day et al. [7] and Jonas and Legras [8] have indicated that the processing of PEEK at high temperatures gives rise to a progressive branching reaction leading to cross-linking. Patel et al. [9] have recently reviewed the

* Corresponding author. Highly Filled Materials Institute, Stevens Institute of Technology, Hoboken, NJ 07030, USA. Tel.: +1 2012168225.
E-mail address: dilhan.kalyon@stevens.edu (D.M. Kalyon).
[1] Present address: Chemical and Biological Engineering Department, Princeton University, NJ 08544, USA.

0032-3861/$ – see front matter © 2010 Elsevier Ltd. All rights reserved.
doi:10.1016/j.polymer.2010.08.060

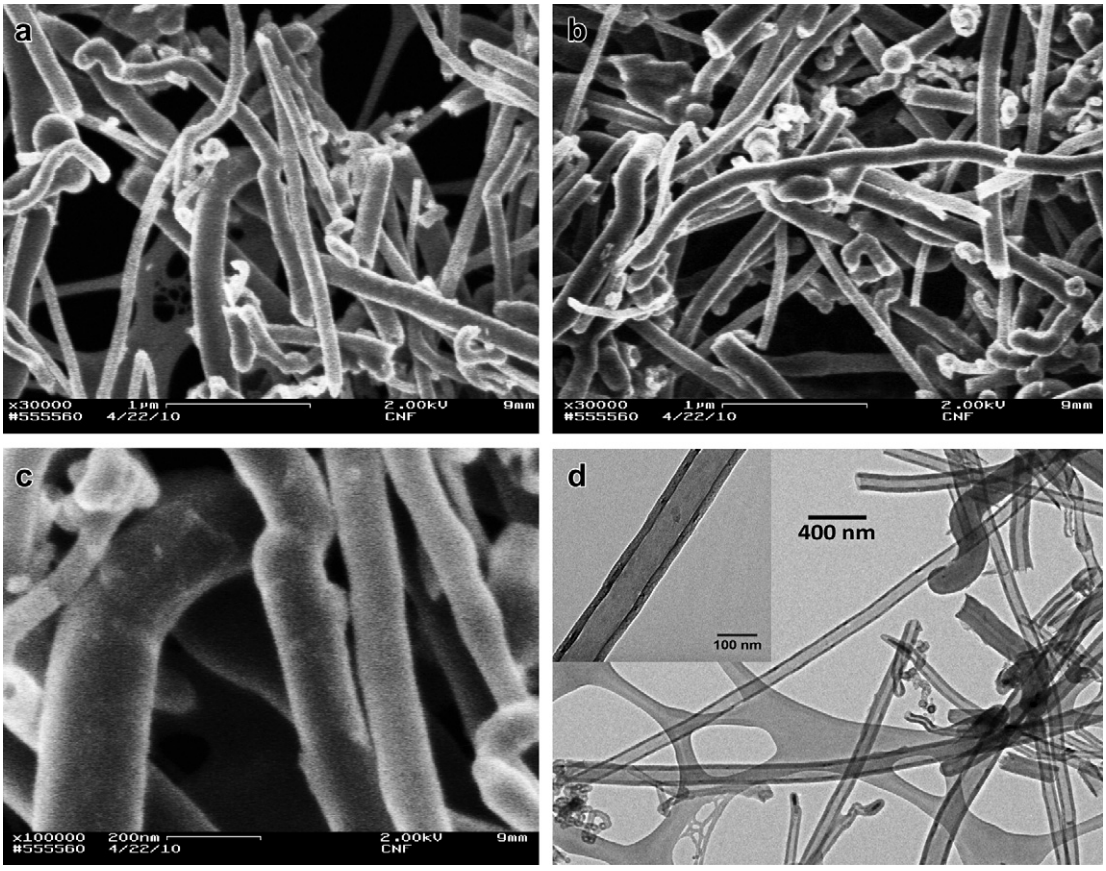

Fig. 1. Carbon nanofibers used in the study (a, b, c: SEM and d: TEM micrographs).

mechanisms of thermal degradation of PEEK along with the generated decomposition products at different temperatures [9].

Carbon nanofibers, CNFs, and carbon nanotubes, CNTs, are widely used in polymer nanocomposites to alter the mechanical, electrical and thermal properties. However, due to difficulties in dispersing of the CNFs and CNTs, specialized methods of compounding CNFs and CNTs into polymers have been investigated, including in situ polymerization techniques [10–12], surface modification of CNTs [13–16], surfactants [17,18], spraying a CNT solution onto a polymeric powder [19], shear-mixing [20], and twin-screw extrusion [21]. Polymers that have been modified with carbon nanofibers for which enhancements of mechanical, electrical or thermal properties are observed, include poly(propylene) [22,23], poly(methyl methacrylate) [24,25], poly(ethylene terepthalate) [26], and poly(carbonate) [27]. The CNFs were found to modify the crystallinity of the PEEK and increase the tensile modulus and yield stress and decrease the solid–solid friction coefficient [21,28–30]. The effects of CNFs and CNTs on the cross-linking behavior of thermosetting polymers have been investigated but the results are controversial and the cross-link density is found to decrease or increase upon the incorporation of the carbon nanofillers [31–38].

The objective of this study is to test two different methods, i.e., solution and melt processing, for the incorporation of CNFs into PEEK and determine the effects of differing processing conditions on the dispersion of CNFs, crystallinity and associated development of the viscoelastic properties of PEEK/CNF nanocomposites. The dynamic properties of the PEEK nanocomposites in the solid and melt phases were collected using small-amplitude oscillatory shear under N_2 and air in the ambient to 400 °C range. The linear viscoelastic material functions are very sensitive to structural changes, i.e., especially to degree of dispersion of the nanoinclusions, crystallinity and oxidative degradation.

2. Experimental

2.1. Materials

Ketaspire PEEK powder (KT-820FP) with a specific gravity of 1.3, supplied by Solvay Advanced Polymers and vapor-grown carbon nanofibers (Fig. 1), supplied by US Army Benét Laboratories (CON2707, PR-19XT-PS-AM), were used in this study. The starting materials were in the form of rigid hollow nanofibers and loose bamboo-like wavy clusters. The diameter and aspect ratio of the rigid nanofibers were 183 ± 24 nm and 39 ± 5, respectively. Benzophenone obtained from Sigma–Aldrich was used as the solvent for solution processing. A nonionic surfactant, Triton X-100, from Sigma–Aldrich was used to aid in the dispersion of the CNFs during processing. The weight percent of CNFs in PEEK was in the 0.1–5% range (volume fraction, ϕ, range of CNFs is 0.0006–0.03).

2.1.1. Solution processing

First carbon nanofibers were sonicated and dispersed in benzophenone with Triton X-100 surfactant at 50 °C using a Misonix XL2020 ultrasonic processor (amplitude of 6 and for 30 min). Samples were collected on glass slides for optical microscopy analysis to evaluate the state of dispersion of the samples following sonication. The benzophenone-CNF suspension was combined with the PEEK powder and heated while stirring to 260 °C. The suspension was stirred for an additional 20 min at 260 °C. The suspension was then cooled to 180 °C, at which point the composite

began to solidify into crumbs. The nanocomposite crumbs were then dried for at least 48 h under vacuum at 190 °C to remove the solvent. Thermo gravimetric analysis, TGA, using a TA Instruments Q50 apparatus, was performed to determine the solvent content after drying. The solvent content after drying was found to be always less than 0.4% by weight. Pure PEEK was also subjected to the same solution processing procedure to allow a fair comparison with the nanocomposites. PEEK/CNF nanosuspensions with CNF incorporated at 0.1–5% by weight (based on the initial weights and also considering the surfactant) were prepared.

2.1.2. Melt processing

The nanofibers were also melt compounded into PEEK using a Haake torque rheometer with a 300 cc mixing head. This is an intensive mixer (a mini Banbury mixer) that has two counter rotating rotors and a temperature controlled barrel and the facility to measure the torque on the shaft, $\Im(t)$, and hence the specific energy, E_a, input during mixing. The mixer was used 70% full. The melt mixing was carried out at a temperature of 380 °C for 30 min. The torque, $\Im(t)$ on the rotating shafts could be measured as a function of time during the mixing of the nanofibers into the PEEK. The specific energy input, E_a, as a function of mixing time, t_m, was determined from:

$$E_a = \Omega \int_0^{t_m} \Im(t)dt/M_t \quad (1)$$

where Ω is the rotational speed of the rotors and M_t is the weight of the suspension that is being mixed in the mixer. The melt mixing was carried out under air, consistent with industrial practice.

2.2. Dynamic properties

During oscillatory shearing of a stable specimen between two disks, one of which is oscillating and the second stationary, the dynamic properties are obtained independent of time. However, if the specimen is not stable for any reason, i.e., cross-linking, hydrolysis, oxidation etc., a time scan whereby the frequency and the strain amplitude are held constant reveals changes in the dynamic properties with time, since the dynamic properties are very sensitive to changes in the structure. In oscillatory shear, the shear strain is defined as $\gamma = \gamma_0 \sin(\omega t)$, where γ_0 is shear strain amplitude (i.e., $\theta D/h$, where θ is the angular displacement, D is the disk diameter and h is the gap in between the two disks), ω is the oscillation frequency and t is the time. The shear stress, τ, response to the imposed oscillatory deformation consists of two contributions associated with the energy stored as elastic energy and energy dissipated as heat, i.e.,

$$\tau = G'(\omega)\gamma_0 \sin(\omega t) + G''(\omega)\gamma_0 \cos(\omega t) \quad (2)$$

where $G'(\omega)$ is the shear storage modulus and $G''(\omega)$ is the shear loss modulus. Overall, $G'(\omega)$ represents the elastic energy stored and $G''(\omega)$ represents the energy dissipated as heat during deformation. In the region of linear viscoelasticity the values of dynamic material properties namely, the storage modulus, $G'(\omega)$, the loss modulus, $G''(\omega)$ and the magnitude of complex viscosity, $\eta^*(\omega) = [(G'/\omega)^2 + (G''/\omega)^2]^{1/2}$, should be independent of the strain amplitude, γ_0.

In our experiments an Advanced Rheological Expansion System (ARES) of TA Instruments was used in conjunction with small-amplitude oscillatory shear experiments. This rheometer consists of an actuator (DC servomotor with a shaft supported by an air bearing with an angular displacement range of 0.05–500 milliradians with a resolution of 0.005 milliradians) to deform the sample under controlled strain conditions and a transducer to measure the normal force and the torque imposed on the sample during the deformation (Force Rebalance Transducer (2K-FRTN1) with a 2000 g-cm torque measurement capability at ±2 g-cm). The chamber temperature could be controlled to within ±0.1 °C and the chamber was flooded with either N_2 (Welco 5.0 Ultra High Purity grade, with $O_2 < 1$ ppm) or compressed air which was dried using Balston in-line filters, i.e., a series of DX, BX and 000 grades, to achieve more than 99.99% removal of moisture and foreign matter.

2.2.1. Dynamic properties of the PEEK melt and PEEK/CNF suspensions

Linear viscoelastic material functions of the PEEK melt and PEEK/CNF suspensions were characterized with the 8-mm parallel disk fixtures for small-amplitude oscillatory shear experiments. The gap between the plates was kept constant at 1 mm. The temperature range investigated was 360–400 °C. The dynamic data were found to be independent of the strain amplitude for strain amplitudes <16% for PEEK and PEEK/CNF nanocomposites. The frequency, ω, range was between 0.1 and 100 rps. For the semi dilute regime the rotary diffusion rate, D_r, at which the nanofibers reorient by Brownian motion becomes: $D_r = 3k_BT\,[\ln(L/d) - 0.8]/(\pi\eta_s L^3)$, where k_B is the Boltzmann constant, T is temperature, L and d are the length and diameter of the nanofibers and, η_s is the shear viscosity of the matrix polymer [39]. For the deformation rates, $\dot{\gamma}$ generated by oscillatory shear at $0.1 \le \omega \le 100$ rps, the Peclet numbers, Pe, for rotation, $Pe = \frac{\dot{\gamma}}{D_r} \gg 1$ indicating that the Brownian motion is negligible. During small-amplitude oscillatory shear, the Reynolds number, Re, is $O(10^{-4})$ indicating that the flow occurs under creeping flow conditions, free of inertial effects.

The use of multiple frequencies allows the characterization of linear viscoelastic response of the dispersions over a range of time scales to provide a broad fingerprint of the viscoelastic response, which would be very sensitive to the state of the dispersion of the CNFs and any type of degradative process. In general, at relatively small characteristic times for deformation (i.e., at high frequencies) the elastic response is accentuated while at longer characteristic times (relatively low frequencies) the viscous response dominates. The storage modulus results are focused on since the storage modulus is especially sensitive to the states of the dispersion achieved during compounding, the cross-link density generated due to thermo-oxidative degradation during mixing and the crystallinity of the moldings.

2.2.2. Rectangular torsional deformation of the PEEK and PEEK/CNF nanocomposites

The dynamic properties of the PEEK and PEEK/CNF nanocomposites were characterized using small-amplitude oscillatory

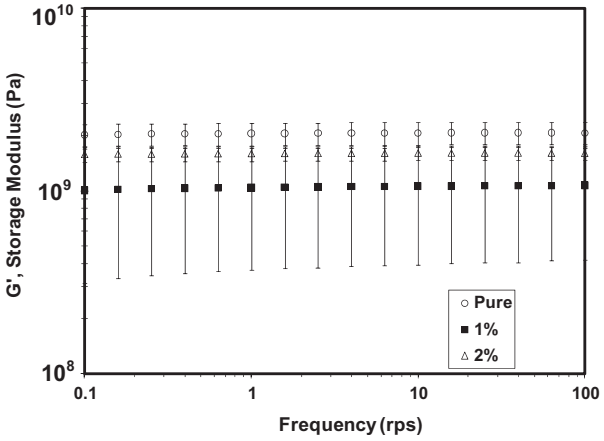

Fig. 2. Storage modulus of melt-compounded PEEK/CNF nanocomposites at ambient temperature.

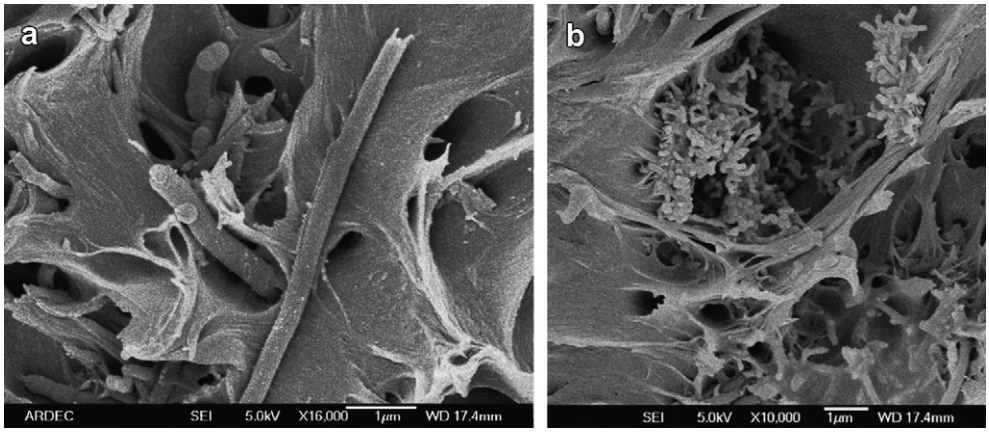

Fig. 3. SEM micrographs of fracture surfaces of melt-compounded PEEK/CNF nanocomposite at 1% by weight CNF.

shear under rectangular torsional deformation at 25–27 °C. The rectangular torsional samples with lengths of 35 ± 5 mm, widths of 9 ± 1 mm and thicknesses of 0.35 ± 0.05 mm were cut from compression-molded sheets of PEEK and PEEK/CNF nanocomposites. During compression molding the melt and solution processed specimens were compressed up to 10,000 psi at a temperature of 400 °C. The cooling for all of the specimens involved a deliberately slow process which involved keeping the specimen compressed in between the two platens (thus without exposure to air) and cooling by free convection until the temperature reached 200 °C. Upon reaching 200 °C the water circulation system of the mold platens was turned on to cool the sample still held in between the two mold platens to ambient temperature within 6 min. The cooling procedure was kept the same for all samples to achieve similar thermal histories. The relatively slow cooling process was preferred so that relatively high crystallinity values could be achieved.

2.3. Differential scanning calorimetry

A TA instruments DSC Q1000 Differential Scanning Calorimeter was used to determine the crystallinity as a function of cooling rate for both the solution and melt processed samples. In these experiments the samples were heated to over 400 °C under a N_2 environment where they were kept for 5 min and then cooled to ambient at various cooling rates in the 2–60 °C/min range. The samples are then heated to 400 °C at a heating rate of 10 °C per minute. The degree of crystallinity of PEEK samples upon exposure to different cooling rates was determined from Degree of crystallinity = $\Delta H_f/\Delta H_{f,p}$, where ΔH_f is the heat of fusion of the sample and $\Delta H_{f,p}$ is the heat of fusion of the pure crystalline PEEK, which is 130 J/g [40]. The heat of fusion, ΔH_f, values were corrected for the presence of the CNFs.

2.4. Thermo gravimetric analysis

Thermal gravimetric analysis, TGA, was carried out using a TA Instruments TGA Q50. The balance mechanism of the TGA unit has a weighing capacity of 1.0 g with accuracy < ±0.1%. During the experiments the PEEK and PEEK nanocomposite samples were placed in platinum pans and were heated from ambient temperature to 800 °C at a rate of 20 °C/min in air.

3. Results and discussion

3.1. Dynamic properties of melt processed samples

The 95% confidence intervals (determined according to Student's t-distribution) of storage modulus, G′, data for pure PEEK and PEEK melt compounded with CNFs at 1 and 2% by weight of CNFs are shown in Fig. 2.

The confidence intervals are generally broad with a negligible effect of the CNFs on the modulus at 1 and 2% by weight (volume

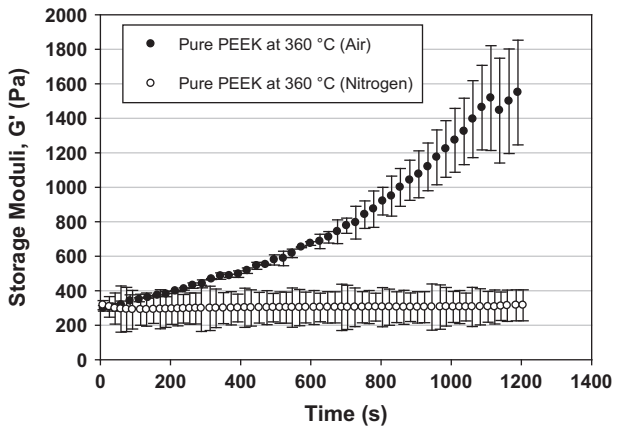

Fig. 4. Storage modulus, G′, versus time under air and N_2 at 360 °C at $\omega = 1$ rps.

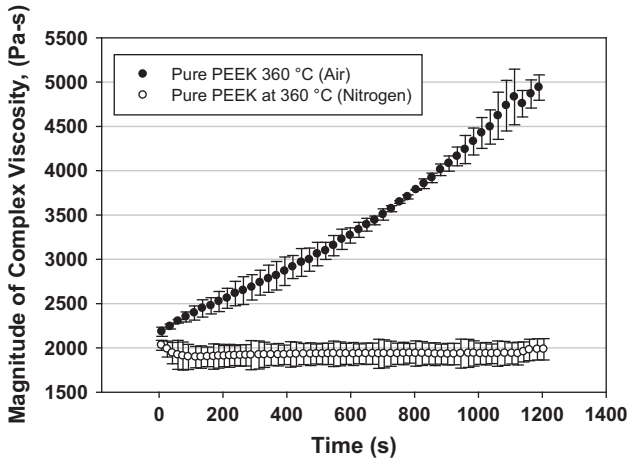

Fig. 5. Magnitude of complex viscosity of PEEK, versus time under air and N_2 at $\omega = 1$ rps.

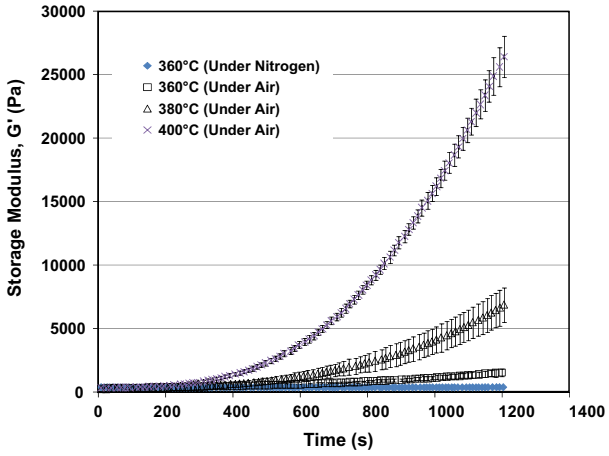

Fig. 6. Storage modulus versus time behavior of PEEK under air and N_2 at different temperatures at $\omega = 1$ rps.

fraction, ϕ of 0.0062 and 0.0125, respectively). A mixing rule can be used for the idealized case of perfect interfacial bonding between the PEEK and CNF to represent the storage modulus of the nanocomposite, G′,

$$G' = f(TMH, \phi)G'_{PEEK}(1-\phi) + g(TMH)G'_{CNF}\phi \quad (3)$$

where ϕ is the volume fraction of the CNFs, G'_{PEEK} is the storage modulus of the PEEK matrix and G'_{CNF} is the storage modulus of the CNF. The function f(TMH, ϕ) represents the effects of the thermo-mechanical history, TMH, and ϕ on crystalline morphology, degree of crystallinity and preferred orientation of the PEEK. The function g (TMH) represents primarily the effects of the thermo-mechanical history on the degree of dispersion and the preferred orientation of the CNFs. The increasing of G′ with increasing ϕ, expected on the basis of Eq. (3), is not at all observed for the melt processed samples of PEEK/CNF nanocomposites as shown in Fig. 2, where the improvement of G′ with increasing ϕ is not observed.

The lack of sensitivity of the G′ data of melt processed PEEK/CNF nanocomposites on ϕ can be based on a number of factors. First, the dispersion could be non-homogeneous. SEM characterization indeed indicated significant differences in dispersion of the nanofibers found at different domains in the nanocomposite samples. For example, the two SEM micrographs of PEEK/CNF nanocomposite samples at 1% by weight of CNFs, shown in Fig. 3 that were obtained upon cryo-fracture suggest very different states of the dispersion of the CNFs.

Fig. 3a which focuses at one location of one specimen of PEEK incorporated 1% by weight the CNFs suggests that the nanofibers are well dispersed into the PEEK matrix. However, Fig. 3b which focuses at a different location of the same specimen (PEEK with 1% by weight CNF) shows an agglomerate of bamboo-like CNFs to suggest that some of the CNFs are poorly wet by the PEEK and remain clustered within the PEEK matrix. Unfortunately, it is not possible to draw a rigorous statistical analysis of the degree of mixedness of the CNFs, as could be carried out on other particle-laden systems [41,42]. Considering that the transition to the concentrated isotropic concentration regime, at which the nanofibers should begin to have difficulty packing isotropically, occurs at $\phi \approx \pi d/4L$ i.e., $O(10^{-2})$ [39], it is not surprising that homogeneity of the dispersion of the CNFs becomes an issue at weight fractions of 1 and 2% (volume fractions, ϕ of 0.0062 and 0.0125).

Would increasing the specific energy input, E_a, incorporated in the melt mixer at temperatures in the 360–400 °C range improve the degree of dispersion of the nanofibers, i.e., increase of t_m or Ω in $E_a = \Omega \int_0^{t_m} \Im(t)dt/M_t$? Figs. 4 and 5 show time-dependent storage modulus and magnitude of complex viscosity data for PEEK at 360 °C collected under air and N_2. When the N_2 environment is used in the chamber of the rheometer there is no change in the dynamic properties of PEEK with time, suggesting that pure PEEK can be assumed to be thermally stable at 360 °C within the 1200 s time span of the experiments. This is consistent with the findings of Day et al. [7] on quiescent PEEK samples (no shearing) which have indicated that PEEK is relatively more stable under an inert gas environment. However, when a similar shearing experiment was carried out under air both the storage modulus, G′(ω), and the magnitude of complex viscosity, η*, values increased significantly with time (Figs. 4 and 5).

The experimental study of Jonas and Legras [8] has revealed that the processing of PEEK at relatively high temperatures "automatically leads to its degradation, even in careful processing conditions". The degradation involves the scission of the PEEK macromolecules, removal of a meta hydrogen with respect to the carboxyl group, formation of PEEK radicals, generation of volatiles and the cross-linking of the PEEK via a progressive branching reaction [7,8]. Thus scission occurs concomitantly with cross-linking, which gives rise to a gel fraction that is insoluble in good solvents of PEEK [8]. The cross-linking is documented via increases of the weight average, M_w, and z-average, M_z, molecular weights. The branching mechanism of PEEK in nitrogen was determined to be slow: only a 10% increase in M_z could be observed after 30 min melting at 440 °C [8]. On the contrary, the branching mechanism was found to be very rapid under air: with M_z increases of >10% observed after 15 min melting at only 385 °C, and of 30% after 30 min melting at 400 °C [8]. The branching rate in air is related to the oxygen diffusion from the surface into the sample and the molecular weight increases occur as functions of the sample surface to volume ratio. Thus, the increases of the storage modulus and magnitude of complex viscosity values with time, observed in Figs. 4 and 5 should be associated with the thermal-oxidative degradation of PEEK, upon which a partially cross-linked network is formed.

The theory of rubber elasticity predicts that the modulus of elasticity is proportional to the number of effective cross-linkages, v_e per volume, V, of the sample [43]. Thus, the increase of the storage modulus, G′(ω), of pure PEEK is associated with the increase of the number of cross-linkages per volume ($\chi_c = v_e/V$), i.e., indicative of the increasing cross-link density of the PEEK [43]. The increasing degree of oxidative cross-linking, χ_c, with time also gives

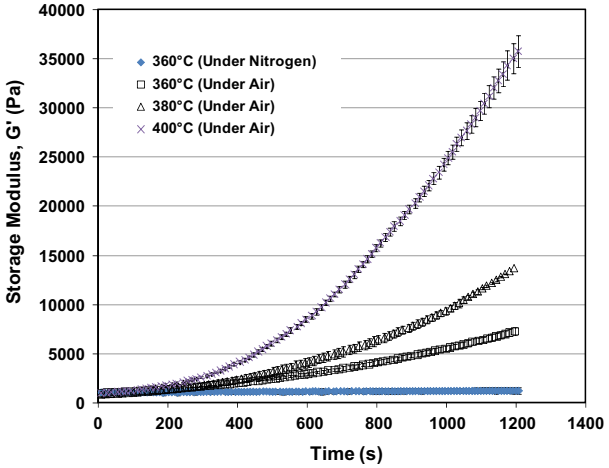

Fig. 7. Storage modulus versus time behavior of solution processed PEEK with 1% by weight CNF under air and N_2 for different temperatures ($\omega = 1$ rps).

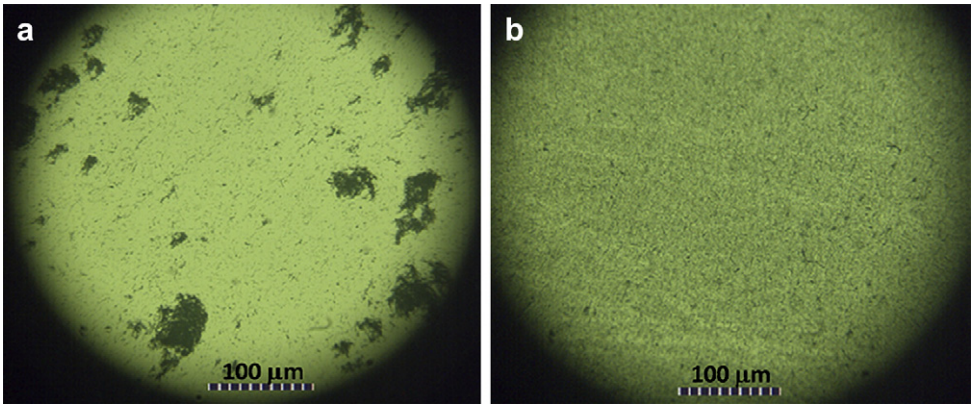

Fig. 8. Optical microscopy of CNF/solvent mixtures, without (Fig. 8a) and with surfactant (Fig. 8b).

rise to the increase of the magnitude of complex viscosity, η*, values of PEEK. Assuming that the storage modulus is directly proportional to the degree of cross-linking [43], i.e.,

$$G'_{PEEK} = A\chi_c \text{ where A is a constant} \quad (4)$$

Eq. (3) becomes (with f(TMH, ϕ) = 1):

$$\frac{dG'(t)}{dt} = (1-\varphi)\frac{dG'_{PEEK}(t)}{dt} = (1-\varphi)A\frac{d\chi_c(t)}{dt} \quad (5)$$

Thus, the positive changes in slope of G′(t) during exposure to high temperatures are indicative of the cross-linking of the PEEK. The temperature dependency of the cross-linking behavior of PEEK is shown in Fig. 6, where the storage moduli are plotted against time at different temperatures. At greater temperatures higher rates of increase of the storage modulus are observed, indicating that the cross-linking process proceeds at significantly higher rates with increasing temperature. The other dynamic properties also exhibit similarly-large increases with time. For example, a 26 fold increase of the magnitude of complex viscosity of PEEK over 20 min is observed at 400 °C.

Fig. 7 shows the time-dependent changes in the storage modulus values of PEEK incorporated with 1% by weight carbon nanofibers under both air and N_2 environments. Under the N_2 environment the nanocomposites of PEEK are also stable, consistent with the findings for pure PEEK. On the other hand, under air, the dynamic properties again increase with time. The increases in dynamic properties are more pronounced at higher temperatures, suggesting again that the PEEK/CNF nanocomposites are also cross-linking significantly under air in a temperature dependent fashion.

Thus, the oxidative degradation, i.e., the cross-linking of the PEEK has been one of the significant contributing factors to the lack of sensitivity of the storage moduli of the PEEK nanocomposites to the volume fraction of the nanofibers, ϕ (Fig. 2). There is a third aspect of structure development upon melt processing that needs to be considered, i.e., both the cross-linking and the dispersion of the nanofibers should affect the crystalline morphology and the degree of crystallinity of the PEEK/CNF nanocomposites. This will be discussed later in section 3.3.

3.2. Dynamic properties of solution processed samples

A second set of PEEK/CNF nanocomposite samples were prepared via solution processing. The surfactant used proved to be quite effective in generating a more homogeneous dispersion of the CNFs in the solvent as shown in Fig. 8.

Significant cluster formation of the CNFs occurs without the benefit of the surfactant (Fig. 8a). The dispersion of the CNFs is

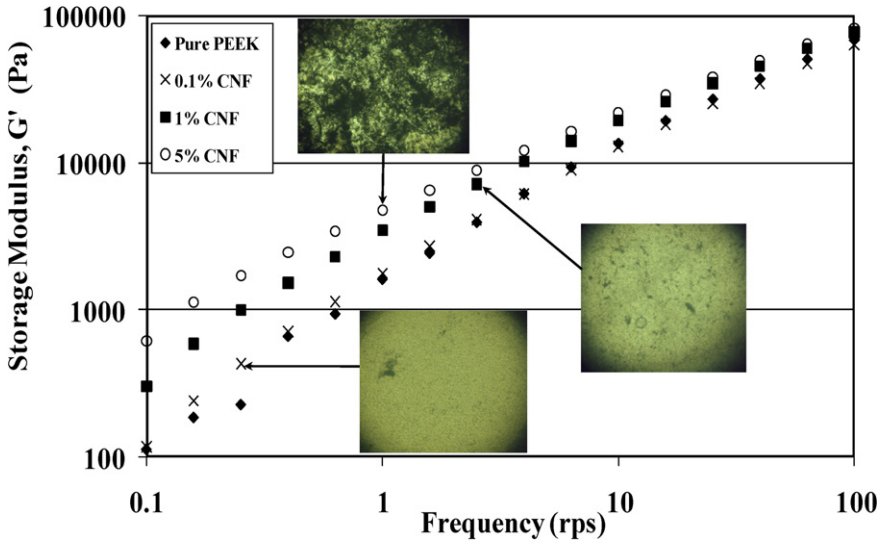

Fig. 9. Storage modulus versus frequency of solution processed PEEK and PEEK/CNF suspensions at 360 °C (insets show optical micrographs of solvent/CNF/PEEK mixtures).

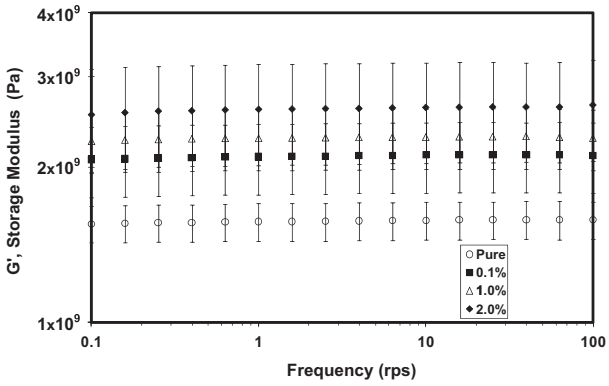

Fig. 10. Storage modulus versus frequency of solution processed PEEK and PEEK/CNF nanocomposites at ambient temperature.

improved considerably upon the use of the surfactant (Fig. 8b). The CNF/solvent mixture was then incorporated into the solution of PEEK, sonicated, the solvent removed by evaporation and then the dynamic properties of the PEEK/CNF nanosuspensions were characterized at a temperature of 360 °C (Fig. 9). The linear viscoelastic material functions of the nanosuspensions are generally related to the dispersion state of the nanoinclusions, with the moduli increasing by orders of magnitude if the nanoinclusions generate a network that spans the entire volume of the sample [44]. The storage and loss moduli of the solution processed PEEK nanocomposites are observed to increase with increasing CNF concentration (see Fig. 9 for G′(ω)). The insets show the typical dispersion states of the nanofibers prior to the removal of the solvent at various concentrations (CNF within the PEEK/benzophenone solution). The increase of the G′ with increasing CNF concentration is only modest, as would be expected on the basis of the relatively low aspect ratios of the nanofibers used in the investigation and the relatively poor states of dispersion of the CNFs as suggested by the insets of Fig. 9.

The storage moduli of the rectangular torsional samples of solution processed PEEK nanocomposite moldings at ambient temperature are shown in Fig. 10. Similar to the behavior of the melt, the G′ values of the solid samples of PEEK/CNF also exhibit sensitivity to the concentration of the CNFs (increasing modulus with increasing concentration of CNF), a sensitivity that could not be observed for the melt processed samples (Fig. 2).

The storage modulus behavior suggests that there are no additional benefits of increasing the concentration of the CNF beyond

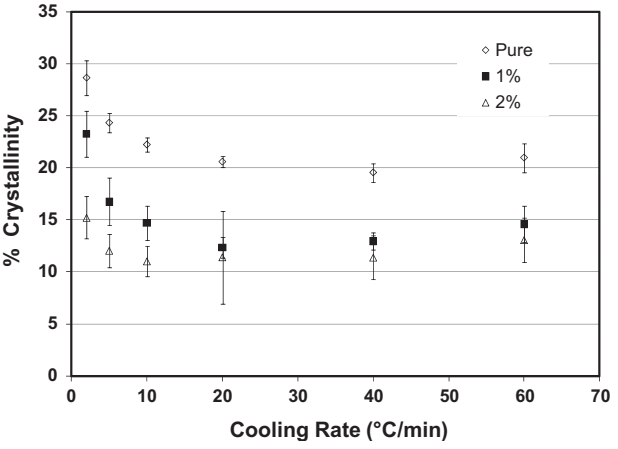

Fig. 11. Crystallinity of solution processed PEEK and PEEK/CNF nanocomposites as a function of cooling rate.

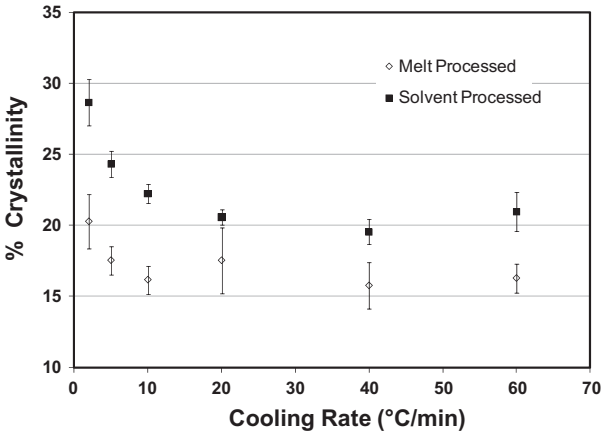

Fig. 12. Crystallinity values of solution vs. melt processed PEEK samples as functions of cooling rate.

2%. For example, PEEK/CNF nanocomposites with 5% by weight CNF exhibited G′ values which were even smaller than those of PEEK with 0.1% by weight CNFs, associated with the difficulty of achieving acceptable dispersions of the nanofibers at concentrations that are above 2%. This is understandable since for the CNFs of this study the concentrated isotropic regime at which the fibers would have difficulty packing isotropically due to excluded volume interactions is onset at a volume fraction of about 0.02 (3% by weight), i.e., $\phi = \pi d/(4L)$ [39]. Thus, even the use of a solution processing method would not be adequate to homogeneously disperse the nanofibers for $\phi > 0.02$.

3.3. Crystallinity

The other factor that plays a role in the development of the viscoelastic properties is the crystallinity of PEEK, i.e., for example, the effects which would increase the crystallinity would also increase the modulus of the composite and vice versa. The degree of crystallinity of solution processed PEEK and PEEK/CNF samples used for the characterization of their dynamic properties indicated that the crystallinity of pure PEEK was 25.8 ± 1.8%, PEEK with 1% by weight CNF was 18.6 ± 3.0% and PEEK with 2% by weight CNF was 12.0 ± 2.5%. Thus, the reinforcement effect of the CNFs is negated to some extent by the decrease of crystallinity associated with the incorporation of the CNFs into the PEEK matrix.

This behavior of decreasing crystallinity with the incorporation of nanoinclusions is in contrast with the findings of previous studies on the crystallization behavior of three other polymers, i.e., poly (vinylidene fluoride), Nylon 11, and poly(butylene terephthalate) incorporated with carbon nanotubes. These studies have shown that the rate of crystallization as well as the ultimate degree of crystallinity of these polymers are favorably affected by the presence of the nanoparticles [45–48]. The principle effect associated with the increase in crystallinity was considered to be the carbon nanoparticles acting as heterogeneous nuclei, thus increasing the rate of nucleation and the rate of crystallization of these three polymers.

The decrease of the crystallinity of PEEK with the incorporation and increasing concentration of CNF is also in contrast to the previous studies of PEEK crystallization in which carbon fibers with greater diameters (versus nanofibers) were utilized. For example, Saleem et al. [49] determined that the crystallinity of PEEK increases from 10% for pure PEEK to 16 and 17% for PEEK incorporated with 10 and 35% of carbon fibers with a diameter of 7 μm and a length over diameter ratio of 860. Furthermore, Sandler et al. [29] determined that the crystallinity of PEEK increased with the

incorporation of CNFs in conjunction with drawn PEEK nanocomposite fibers in which the CNFs were uniaxially well-aligned along the fiber draw direction [29]. With these drawn fibers, the degree of crystallinity of PEEK increased from 6% to 12% when 5% of CNFs were incorporated but PEEK crystallinity remained constant upon changes in the concentration of the CNFs from 5 to 10% [29]. No heterogeneous nucleation effect of the CNFs on PEEK was observed and the increase of crystallinity appears to be associated with the ordering induced by the preferred orientation of the nanofibers [29]. In our processing such uniaxial preferred orientation of the rigid nanofibers is absent. In the absence of heterogeneous nucleation and preferred orientation effects, the presence of the unoriented rigid CNFs with relatively low aspect ratios would render it more difficult for the PEEK chains to undergo the folding requisite for crystallization, thus reducing the rate of crystallization and consequently the degree of crystallinity.

The decrease of the degree of crystallinity of PEEK upon the incorporation of CNFs is further observed in DSC experiments involving the determination of crystallinity as a function of the cooling rate (Fig. 11). The degree of crystallinity of PEEK decreases with increasing cooling rate in differential scanning calorimetry, consistent with earlier studies on other polymers [50,51]. The crystallinity values of solution processed PEEK nanocomposites at 0, 1 and 2% by weight of CNF indicate that, consistent with the crystallinity values of the moldings of solution processed samples, the crystallinity of PEEK decreases with the incorporation of fibrous nanoinclusions.

The comparisons of the crystallinity versus cooling rate behavior of PEEK subjected to the melt and solution processing methods used in the compounding of the CNF into PEEK are shown in Fig. 12. The solution processed PEEK samples exhibit higher crystallinity values in comparison to melt processed samples. As discussed earlier, since the melt mixing was carried out for 30 min under air at 400 °C the melt mixed PEEK is cross-linked. Such cross-linking gives rise to a significant increase in the shear viscosity of PEEK, which should hinder the self-assembly of the macromolecules for crystallization, thus decreasing the rate of crystallization; a finding which is consistent with the earlier study of Jonas and Legras [8] on the effects of cross-linking on the crystallization of PEEK. Thus, the storage moduli data of melt processed PEEK nanocomposites shown in Fig. 2 are affected by the state of the dispersion of the CNFs, the thermal-oxidative degradation associated with the high temperatures and residence times involved in melt processing and the adverse effects of cross-linking on the development of the crystallinity. The complex interactions between the myriad factors of processing thus significantly complicate the utilization of nanoinclusions for the enhancement of the ultimate properties of engineering polymers.

Thermogravimetric analysis of the solution processed samples (results not shown) indicated that thermal stability of PEEK improved slightly upon the incorporation of CNFs. The mean temperature at which 50% weight loss occurs at 1% was about 2 °C higher than at 0% and 2 °C higher at 2% in comparison to 1%. However, the scatter in the data was considerable. In contrast carbon nanotubes significantly improve the thermal stability of nanocomposites [52]. It appears that the relatively low aspect ratios of the CNFs of our study do not enable the formation of an effective volume-spanning network to act as a heat shield that is possible with the higher aspect ratio nanotubes.

4. Conclusions

Two different processing methods were used to prepare nanocomposites of poly(ether ether ketone), PEEK, and carbon nanofibers, CNF. The linear viscoelastic properties of nanocomposite samples prepared via melt processing exhibited no sensitivity to the concentration of the CNFs. This was attributed to the poor dispersion of the CNFs as well as the oxidative cross-linking of the PEEK during melt processing under air at 380 °C. The oxidative cross-linking also leads to a decrease of the crystallinity of the PEEK/CNF nanocomposites. The solution processed PEEK/CNF nanocomposites provided better (but by no means ideal) dispersions. Consequently the viscoelastic properties of the PEEK suspensions exhibited increased elasticity and viscosity with increasing concentration of CNFs up to 2%. At higher CNF concentrations the homogeneity of the dispersions achieved with solution processing also became very poor due to the difficulty of the nanofibers to pack isotropically. In contrast to the previous reports with other polymers and earlier studies of PEEK with carbon fibers and oriented CNFs, the presence of the carbon nanofibers within the PEEK matrix gave rise to a decrease of the crystallinity of the PEEK, presumably associated with the steric hindrance resulting from the presence of the rigid nanofibers.

Acknowledgements

The investigation was funded by Benét Laboratories/ARDEC for which we are grateful. We thank Ms. Asli Ergun, Ms. Seda Vural and Mr. Daniel Ward for their help with some of the experiments.

References

[1] De Bartolo L, Morelli S, Rende M, Gordano A, Drioli E. Biomaterials 2004;25(17):3621–9.
[2] Toth J, Wang M, Estes B, Scifert J, Seim III H, Turner A. Biomaterials 2006;27(3):324–34.
[3] Rae PJ, Brown EN, Orler EB. Polymer 2007;48:598–615.
[4] Day M, Suprunchuk T, Cooney JD, Wiles DM. J Appl Poly 1988;36:1097.
[5] Chan CM, Venkatraman S. J Appl Poly Sci; 1986:32.
[6] Day M, Cooney JD, Wiles DM. J Appl Poly 1989;38:189–97.
[7] Day M, Sally D, Wiles DM. J Appl Poly 1990;40:163–73.
[8] Jonas AM, Legras R. Polymer 1991;32:2691–706.
[9] Patel P, Hull TR, McCabe RW, Flath D, Grasmeder J, Percy M. Poly Degrad Stabil 2010;95:709–18.
[10] Mitchell CA, Bahr JL, Arepalli S, Tour JM, Krishnamoorti R. Macromolecules 2002;35:8825–30.
[11] Fukushima T, Kosaka A, Yamamoto Y, Aimiya T, Notazawa S, Takigawa T, et al. Small 2006;2:554–60.
[12] Zhu B, Xie S, Xu Z, Xu Y. Comp Sci Tech 2006;66:548–54.
[13] Mitchell CA, Krishnamoorti R. Macromolecules 2007;40:1538–45.
[14] Hobbie EK, Fry DJ. J Chem Phys 2007;126(124907):1–7.
[15] Abdalla M, Dean D, Adibempe D, Nyairo E, Robinson P, Thompson G. Polymer 2007;48:5662–70.
[16] Shanmugharaj AM, Bae JH, Lee KY, Noh WH, Lee SH, Ryu SH. Comp Sci Tech 2007;67:1813–22.
[17] Gong X, Liu J, Baskaran S, Voise RD, Young JS. Chem Mater 2000;12:1049–52.
[18] Gojny FH, Schulte K. Comp Sci Tech 2004;64:2303–8.
[19] Zhang Q, Lippits DR, Rastogi S. Macromolecules 2006;39:658–66.
[20] Andrews R, Jacques D, Minot M, Rantell T. Macromol Mater Eng 2002;287:395–403.
[21] Werner P, Altstädt V, Jaskulka R, Jacobs O, Sandler JKW, Shaffer MSP, et al. Wear 2004;257:1006–14.
[22] Kruiger RJ, Alam K, Anderson DP. J Mater Res 2001;16:226–32.
[23] Lozano K, Barera EV. J Appl Polym Sci 2001;79:125–33.
[24] Cooper CA, Ravich D, Lips D, Mayer D, Wagner H. Composites Sci Technol 2002;62:1105–12.
[25] Zeng J, Saltysiak B, Johnson WS, Schiraldi DA, Kumar S. Composites Part B Eng 2004;35:245–9.
[26] Ma H, Zeng J, Kumar S, Schiraldi D. Composites Sci Technol 2003;63:1617–28.
[27] Higgins BA, Brittain WJ. Eur Polym J 2005;41:889–93.
[28] Sandler J, Werner P, Shaffer MSP, Demchuk V, Altstädt V, Windle AH. Composites Part A: Appl Sci Manufacturing 2002;33:1033–9.
[29] Sandler J, Windle AH, Werner P, Altstadt V, Es MV, Shaffer MSP. J Mater Sci 2003;38:2135–41.
[30] Werner P, Verdejo R, Wöllecke F, Altstädt V, Sandler JKW, Shaffer MSP. Adv Mater 2005;17:2864–9.
[31] Bae J, Jang J, Yoon SH. Macromol Chem Phys 2002;203:2196.
[32] Puglia D, Valentini L, Armentano I, Kenny JM. Diamond Relat Mat 2003;12:827.
[33] Fidelus JD, Wiesel E, Gojny FH, Schulte K, Wagner HD. Composites Part A 2005;36:1555–61.

[34] Xiao KQ, Zhang LC. J Mater Sci 2005;40:6513–6.
[35] Tao K, Yang S, Grunlan JC, Kim Y, Dang B, Deng Y, et al. App Polym Sci 2006;102:5248–54.
[36] Wang S, Liang Z, Liu T, Wang B, Zhang C. Nanotechnology 2006;17:1551–7.
[37] Zhou Y, Pervin F, Lewis L, Jeelani S. Mater Sci Eng A 2007;452–453:657–64.
[38] Zhou T, Wang X, Liu X, Xiong D. Carbon 2009;47:1112–8.
[39] Larson RG. The structure and rheology of complex fluids. New York: Oxford University Press; 1999.
[40] Blundell DJ, Osborn BN. Polymer 1983;24(8):953–8.
[41] Kalyon DM, Birinci E, Yazici R, Karuv B, Walsh S. Polym Eng Sci 2002;42:1609–17.
[42] Yazici R, Kalyon DM. Rubber Chem Tech 1993;66:527–37.
[43] Flory P. Principles in polymer chemistry. Ithaca, NY: Cornell Univ. Press; 1953.
[44] Vural S, Dikovics K, Kalyon DM. Soft Matter 2010;6:3870–5.
[45] Mago G, Fisher FT, Kalyon DM. Macromolecules 2008;41:8103–13.
[46] Mago G, Kalyon DM, Fisher FT. Polym Mater Sci Eng 2008;99:508.
[47] Mago G, Fisher FT, Kalyon DM. J Nanoscience Nanotechnology 2009;9:3330–40.
[48] Mago G, Fisher FT, Kalyon DM. J Appl Polym Sci 2009;114:1312–9.
[49] Saleem A, Frormann L, Iqbal A. Polym Composites 2007;28:785–96.
[50] Kamal M, Kalyon DM, Dealy J. Polym Eng Sci 1980;20:1117–26.
[51] Kamal M, Kalyon DM. Polym Eng Sci 1983;23:503–9.
[52] Kashiwagi T, Harris Jr RH, Zhang X, Briber RM, Cipriano BH, Raghavan SR, et al. Polymer 2004;45:881–91.